Environmental Science and Ecotechnology 21 (2024) 100438

Contents lists available at ScienceDirect

Environmental Science and Ecotechnology

journal homepage: www.journals.elsevier.com/environmental-science-and-ecotechnology/

Original Research

Nitrite-driven anaerobic ethane oxidation

Cheng-Cheng Dang [a], Yin-Zhu Jin [a], Xin Tan [a], Wen-Bo Nie [b], Yang Lu [c], Bing-Feng Liu [a], De-Feng Xing [a], Nan-Qi Ren [a], Guo-Jun Xie [a, *]

[a] State Key Laboratory of Urban Water Resource and Environment, School of Environment, Harbin Institute of Technology, Harbin, 150090, China
[b] Key Laboratory of the Three Gorges Region's Eco-Environment, Ministry of Education, College of Environment and Ecology, Chongqing University, Chongqing, 400044, China
[c] Water Innovation and Smart Environment Laboratory, School of Civil and Environmental Engineering, Faculty of Engineering, Queensland University of Technology, Brisbane, Queensland, 4001, Australia

ARTICLE INFO

Article history:
Received 9 January 2024
Received in revised form
8 June 2024
Accepted 8 June 2024

Keywords:
Anaerobic ethane oxidation
Denitrification
Microbial culture
Fumarate addition pathway
Greenhouse gas

ABSTRACT

Ethane, the second most abundant gaseous hydrocarbon in vast anoxic environments, is an overlooked greenhouse gas. Microbial anaerobic oxidation of ethane can be driven by available electron acceptors such as sulfate and nitrate. However, despite nitrite being a more thermodynamically feasible electron acceptor than sulfate or nitrate, little is known about nitrite-driven anaerobic ethane oxidation. In this study, a microbial culture capable of nitrite-driven anaerobic ethane oxidation was enriched through the long-term operation of a nitrite-and-ethane-fed bioreactor. During continuous operation, the nitrite removal rate and the theoretical ethane oxidation rate remained stable at approximately 25.0 mg NO_2^-N L^{-1} d^{-1} and 11.48 mg C_2H_6 L^{-1} d^{-1}, respectively. Batch tests demonstrated that ethane is essential for nitrite removal in this microbial culture. Metabolic function analysis revealed that a species affiliated with a novel genus within the family Rhodocyclaceae, designated as '*Candidatus* Alkanivoras nitrosoreducens', may perform the nitrite-driven anaerobic ethane oxidation. In the proposed metabolic model, despite the absence of known genes for ethane conversion to ethyl-succinate and succinate-CoA ligase, '*Ca.* A. nitrosoreducens' encodes a prospective fumarate addition pathway for anaerobic ethane oxidation and a complete denitrification pathway for nitrite reduction to nitrogen. These findings advance our understanding of nitrite-driven anaerobic ethane oxidation, highlighting the previously overlooked impact of anaerobic ethane oxidation in natural ecosystems.

1. Introduction

Ethane is an overlooked greenhouse gas; its global warming potential is 12.8 times that of carbon dioxide (CO_2) [1]. Ethane is the second most abundant short chain alkane in natural gas. Nature gas exploitation and crude oil refining have led to significant anthropogenic ethane emissions, accounting for ~60% of global ethane emissions [2,3]. Thus, ethane is a tracer for natural gas fugitive emissions [4,5]. Burning fossil fuels and biofuels is another important ethane emission source [3,6]. Biological and abiotic ethane production has also been widely observed in natural environments, such as hydrothermal vent fluids [7], hydrothermally heated sediments [8], deep marine sediments [9], and cyanobacteria isolated from hot springs [10]. Accordingly, global ethane emissions have been as high as 18.7 Tg yr^{-1} [2] and have significantly contributed to global climate change. Ethane emissions may also lead to ozone layer depletion, atmospheric voids, and photochemical pollution because ethane is a precursor for photochemical reactions [11].

Fortunately, geochemical profile data suggest that microbial activity reduces the emissions of short-chain alkanes in anaerobic or hypoxic environments [12,13]. Anaerobic ethane oxidation was found in mud volcanoes in the Nile deep-sea fan with other short-chain hydrocarbon gas oxidation [12]. For instance, bacteria affiliated with Deltaproteobacteria, particularly sulfate-reducing lineage, were predicted to mediate anaerobic ethane oxidation and sulfate reduction in hydrothermal vent and mud volcano sediment [14,15]. A previously described propane-oxidizing '*Candidatus* Alkanivorans nitratireducens' has been demonstrated to perform nitrate-driven anaerobic ethane oxidation [16]. These findings

* Corresponding author.
E-mail addresses: xieguojun0707@163.com, xgj@hit.edu.cn (G.-J. Xie).

https://doi.org/10.1016/j.ese.2024.100438

elucidate the overlooked role of ethane in linking several global biogeochemical cycles.

Several studies have revealed the mechanism of microbial sulfate or nitrate-driven anaerobic ethane oxidation through biomass cultivation and meta-omics analysis [16–19]. Thus, archaea activate and oxidize ethane through ethyl-coenzyme M (ethyl-CoM) reductase, and sulfate-reducing partner bacteria are associated with these archaea for receiving electrons [17–19]. The subsequent oxidation to CO_2 was achieved through the reverse Wood–Ljungdahl pathway. In addition, bacteria could independently complete anaerobic ethane oxidation by synchronously reducing nitrate to nitrogen (N_2) [16]. A prospective fumarate addition pathway is crucial for ethane oxidation in bacteria [16,20], although the detailed mechanism requires further explanation. Nitrite is a common electron acceptor in freshwater ecosystems [21], which can coexist with ethane in hot springs [22,23]. As a potential electron acceptor for anaerobic ethane oxidation, nitrite is more thermodynamically feasible than sulfate and nitrate (equation (1)–(3)). However, whether nitrite-driven anaerobic ethane oxidation exists remains unclear.

$$4C_2H_6 + 7SO_4^{2-} \rightarrow 7S^{2-} + 8\ CO_2 + 12\ H_2O\ \Delta G^{\circ\prime} = -318.3\ \text{kJ per mol}\ C_2H_6 \quad (1)$$

$$5C_2H_6 + 14NO_3^- \rightarrow 7N_2 + 14OH^- + 10\ CO_2 + 8\ H_2O\ \Delta G^{\circ\prime} = -1160.6\ \text{kJ per mol}\ C_2H_6 \quad (2)$$

$$3C_2H_6 + 14NO_2^- \rightarrow 7N_2 + 14OH^- + 6\ CO_2 + 8\ H_2O\ \Delta G^{\circ\prime} = -1521.0\ \text{kJ per mol}\ C_2H_6 \quad (3)$$

This study used a bioreactor inoculated with hot-spring sediments to enrich and characterize the microbial culture that mediates nitrite-driven anaerobic ethane oxidation. We employed 16S rRNA gene amplicon sequencing to investigate microbial community changes during long-term reactor operation. Metagenomics and metatranscriptomics analysis identified functional microorganisms and related metabolic mechanisms. The bacteria '*Candidatus* Alkanivoras nitrosoreducens' encoded a prospective fumarate addition pathway for anaerobic ethane oxidation and a complete denitrification pathway for nitrite reduction to nitrogen. These findings significantly advance our understanding of nitrite-driven anaerobic ethane oxidation.

2. Materials and methods

2.1. Bioreactor configuration, inoculum, and enrichment

A lab-scale membrane-bound expanded granular sludge bed (M-EGSB) fed with ethane and nitrite was employed to enrich the bacterial cultures. Reactor configurations and schematic diagrams are provided in Text S1 and Fig. S1 (Supplementary Material). The pressure of supply gas (v/v: 95% C_2H_6/5% CO_2) was maintained at ~0.1 MPa by a gas regulator (GENTEC, China). Fresh hot-spring sediment collected from Tangyu, Shaanxi province, China, was used as inoculum. The sediment was transformed into slurry by adding a synthetic mineral medium (the composition refers to Supplementary Material Text S2).

A total of 500 mL of slurry was injected into the reactor after filtration through a screen. The bioreactor was operated in the start-up stage (Phase I: days 0–86) and the continuous stage (Phase II: days 87–350). During the start-up phase, the microbial culture capable of nitrite-driven anaerobic ethane oxidation was cultivated through a pulsed supply of nitrite. Then, a stable continuous nitrite supply was provided to accelerate the enrichment of microorganisms. From days 87–211, the influent nitrite concentration was maintained at 100 mg NO_2^--N L^{-1}, and the nitrite loading rate in the bioreactor was increased by shortening the hydraulic retention time (HRT) in stages. From days 212–350, the influent nitrite concentration was increased to 500 mg NO_2^--N L^{-1} to avoid microbial biomass loss. A peristaltic pump (BT600s, Lead Fluid, China) maintained internal recirculation and the complete mixture. A water jacket was used for stabilized temperature control at 45 ± 0.5 °C. The system's pH was monitored by a pH meter (AZ Co., Ltd., China) and maintained at 6.5–7.5 by manually injecting 1 M HCl or 1 M NaOH solutions.

2.2. Batch tests to verify ethane metabolism

Batch tests for checking the ethane metabolism were performed on biomass inoculated from the M-EGSB, with 200 mL of anaerobic synthetic culture medium and 50 mL of microbial culture inoculated into two 510 mL continuous stirred-tank reactors (CSTR). Then, both CSTRs were immediately aerated with a mixed gas (v/v: 95% argon [Ar]/5% CO_2) for 15 min to maintain an anaerobic environment. The CSTRs were divided into experimental groups (flushed with 95% C_2H_6 and 5% CO_2 for 10 min) and control groups (flushed with 95% Ar and 5% CO_2 for 10 min). Nitrite was added to the experimental and control groups to produce a final concentration of about 10 mg N L^{-1}. Liquid samples were collected every 20 min, and the nitrite concentration was analyzed over 2 h. All batch tests were repeated in triplicate.

2.3. DNA extraction and 16S rRNA gene amplicon sequencing

The biomass samples were collected from the bioreactor and stored at −80 °C. The total genomic DNA was extracted using the OMEGA Soil DNA Kit (M5636-02, Omega Bio-Tek, USA). The quantity and quality of the extracted DNAs were measured using a NanoDrop NC2000 spectrophotometer (Thermo Fisher Scientific, USA) and agarose gel electrophoresis. The Bact341F-Bact805R primer pair was used to amplify the bacterial V3–V4 region (Supplementary Material Table S1). Amplicon bacterial libraries were sequenced on the Illumina Mi-Seq PE300 high-throughput platform (Illumina, USA) at Sangon Biotech (Shanghai, China). After sequencing, the adapters and primer sequences were clipped from the retrieved sequences using the DADA2 plugin [24]. After the sequences were quality filtered, denoised, and merged, and the chimera was removed, they were assigned to amplicon sequence variant (ASVs) and identified taxonomy using the DADA2 plugin against the SILVA Release v138.1 [25]. For ASVs with incomplete taxonomy information, KEGG Blast was used for manual correction (*https://www.genome.jp/tools/blast*). The raw sequence data was deposited in the Genome Sequence Archive at the National Genomics Data Center (GSA: CRA014268). They are publicly accessible at

https://ngdc.cncb.ac.cn/gsa [26,27].

2.4. Metagenomic DNA extraction, sequencing, and analysis, and genome recovery

Biomass samples were collected from the bioreactor, immediately frozen using liquid nitrogen, and stored at −80 °C on days 150, 250, and 350. Metagenome shotgun sequencing was performed at Personal Biotechnology (Shanghai, China). Metagenomic DNA extraction, sequencing, and DNA library construction are described in Supplementary Material Text S3**.** Metagenomic shotgun sequencing reads were analyzed on the KBase platform [28]. The methods for metagenomic raw data processing and genome recovery are described in Supplementary Material Text S4. Metagenomic reads were mapped to the obtained metagenomic assembly by DiTing v0.9 to determine the relative abundance of metabolic pathways [29], which was calculated as genes per kilobase million (GPM) values (Supplementary Material Data Set S1). The metagenomic reads were aligned with the metagenomic assembly using Bowtie2 v2.3.2, and then relative gene abundance were calculated using StringTie v2.1.5 [30,31]. Redundant metagenome-assembled genomes (MAGs) were dereplicated with dRep v2.3.2 using the dereplicate_wf [32].

Metagenomic assembly data were annotated using Prokka v1.14.5, and MAGs were annotated using RASTtk v1.073 [33,34]. All MAGs were taxonomically classified with GTDB-Tk v1.7.0 [35]. The average nucleotide identity (ANI) of MAGs was calculated by FastANI [36]. The nucleotide sequences of genes encoding alkylsuccinate synthase (KEGG database, Dalk_1731 AssA1, Dalk_2199 AssA2) were aligned with nucleotide sequences of metagenomes and all MAGs using usearch (Version 11) to detect known alkylsuccinate synthase genes [37]. The MAGs were reannotated using the DRAM plugin (default parameters) on the KBase platform [28,38] to identify the core metabolism and key genes involved in prospective nitrite-driven anaerobic ethane oxidation. A species tree was constructed by the Insert Set of Genomes into SpeciesTree plugin v2.2.0 using a set of 49 core, universal genes defined by clusters of orthologous groups gene families [28]. The species tree was optimized using MEGA11 [39].

2.5. Extraction of RNA, shotgun sequencing, and reads processing

The metatranscriptomic sample was collected from the bioreactor, immediately frozen using liquid nitrogen, and then stored at −80 °C on day 250. The total RNA was extracted using an RNA PowerSoil® Total RNA Isolation Kit (12866-25, MoBio, USA). The integrity of RNA was detected using an Agilent 2100 (Agilent, USA). After removing ribosomal RNA from the microbial RNA, the TruSeq Stranded mRNA LT Sample Prep Kit (Illuminia, USA) was used for reverse transcription and macro-transcriptome birdshot sequencing library construction. Each library was sequenced using the Illumina NovaSeq platform (Illumina, USA) with the PE150 strategy at Personal Biotechnology Co., Ltd. (Shanghai, China).

Metatranscriptomic sequencing reads were analyzed on the KBase platform [28]. The RNA paired-end reads were quality controlled by Trimmomatic v0.36 [40]. The quality of trimmed reads was assessed using FastQC [41]. Quality-controlled RNA reads were mapped to the obtained metagenomic assembly by DiTing v0.9 to determine the relative abundance of metabolic pathways [29], which were calculated as transcripts per million (TPM) (Supplementary Material Data Set S1). The quality-controlled RNA reads were also aligned with the corresponding metagenome using Bowtie2 v2.3.2, and then assembled into transcripts for which relative abundance was calculated using StringTie v2.1.5 [30,31]. The metatranscriptomic paired RNA reads library was mapped to potential functional MAGs (recovered from the metagenome collected on day 250) to determine the relative transcriptional abundance of genes involved in denitrification (nitrite to N_2), the prospective fumarate addition pathway, and the reverse Wood−Ljungdahl pathway. The raw metagenomic and metatranscriptomic sequence data were deposited in the Genome Sequence Archive at the National Genomics Data Center (GSA: CRA014262) and are publicly accessible at https://ngdc.cncb.ac.cn/gsa [26,27].

2.6. Routine chemical analytic methods

Liquid samples were filtered through a Millipore filter (0.45 μm pore size) and immediately subjected to routine chemical analysis. Concentrations of nitrite (APHA-4500-NO_2^- B and APHA-4500-NO_3^- B) were measured using standard methods [42], and concentrations of NH_4^+-N were measured using the Nessler method [43]. An Agilent 7890A (Agilent, USA) gas chromatograph equipped with an electron capture detector was used to measure the concentrations of ethane, nitrogen gas, and methane in the reactor exhaust gas.

3. Results and discussion

3.1. Enrichment and performance of nitrite-driven anaerobic ethane oxidation microbial culture

Long-term reactor operation was employed to enrich the

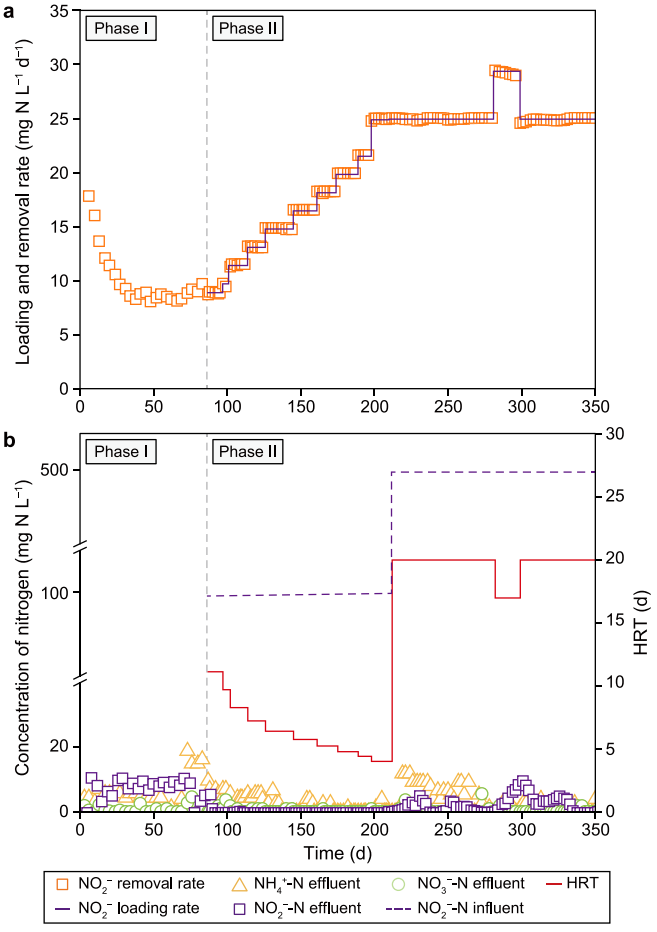

Fig. 1. Reactor performance during 350 days of operation. **a**, Nitrite loading rate and removal rate. **b**, HRT, the nitrite concentration in influent, and the concentrations of nitrate, nitrite, and ammonium in effluent. Phase I indicates the start-up stage; Phase II indicates the continuous stage.

microbial culture capable of nitrite-driven anaerobic ethane oxidation and to investigate its nitrogen removal performance (Fig. 1). A pulsed supply of nitrite was used to cultivate nitrite-driven anaerobic ethane-oxidizing microorganisms during the start-up stage. The nitrite removal rate in the reactor gradually decreased from 17.8 to 8.1 mg NO_2^--N L^{-1} d^{-1} in 0–48 days. It was speculated that nitrite was mostly removed by heterotrophic denitrifying microorganisms during this time, while some microorganisms decayed to produce organic matter for denitrification.

Subsequently, the nitrite removal rate remained stable but slightly increased from days 48–85. After 86 days, a continuous nitrite supply was used to enrich the microbial culture. From days 86–210, the HRT stepwise decreased from 11.1 to 4.0 d, and the nitrite loading rate stepwise increased from 9.0 to 25.0 mg NO_2^--N L^{-1} d^{-1}. Accordingly, the nitrite removal rate gradually increased from 8.7 to 25.0 mg NO_2^--N L^{-1} d^{-1} in the bioreactor, where the nitrite concentration in the effluent was nearly below the detection limit. However, the decrease in HRT resulted in a washout of biomass. To avoid biomass loss, the nitrite concentration in the influent was increased from 100 to 500 mg NO_2^--N L^{-1} on day 210, and the HRT was increased from 4.0 to 20.0 d to maintain the nitrite loading rate at 25.0 mg NO_2^--N L^{-1} d^{-1}. During continuous operation, the nitrite removal rate was stable at about 25.0 mg NO_2^--N L^{-1} d^{-1} from days 198–350. The corresponding theoretical ethane oxidation rate was calculated using equation (3), which was stable at about 11.48 mg C_2H_6 L^{-1} d^{-1} (Supplementary Material Fig. S2). Moreover, the flocculent biomass showed significant growth during the reactor's entire operation (Supplementary Material Fig. S3). These results indicated that microorganisms performing nitrite-driven anaerobic ethane oxidation were likely enriched in the bioreactor.

Batch experiments investigated the relationship between ethane metabolism and nitrite reduction (Fig. 2). When supplying ethane, the nitrite concentration decreased from 9.73 to 1.66 mg NO_2^--N L^{-1} in 2 h. However, when ethane was replaced with the inert gas Ar, the nitrite concentration decreased from 9.77 to 8.90 mg NO_2^--N L^{-1} in 2 h. The average nitrite removal rate reached 4.03 mg NO_2^--N L^{-1} h^{-1} with ethane, much higher than without ethane. Since ethane was the only available electron donor in batch experiments, these results suggest the occurrence of nitrite-driven anaerobic ethane oxidation, and the electrons required for nitrite reduction may be generated from ethane oxidation.

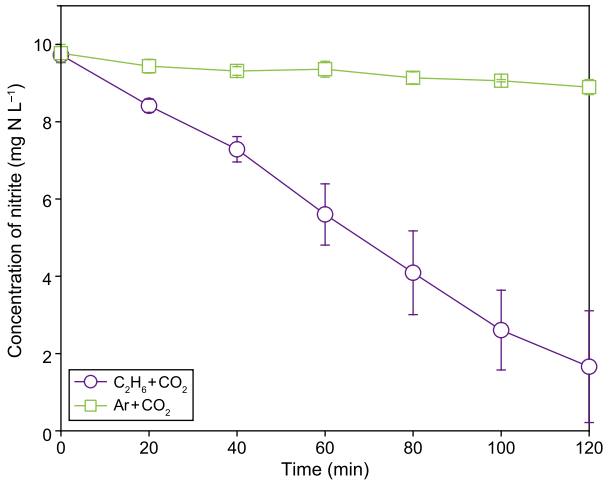

Fig. 2. Nitrite removal performance in batch tests on day 209. Circles: 95% C_2H_6 + 5% CO_2 in headspace; squares: 95% Ar + 5% CO_2 in headspace.

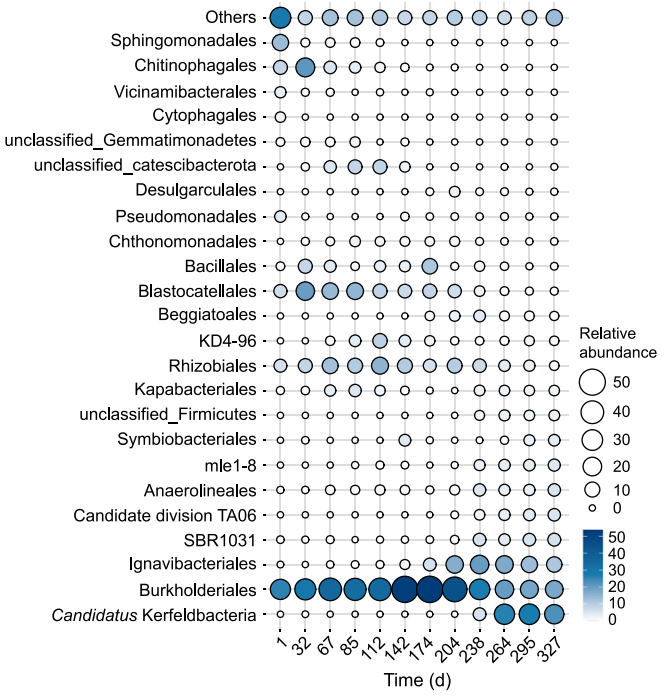

Fig. 3. Microbial community changes during long-term operation. Relative order-level abundance of microbial population (>2% in at least one sample) was shown.

3.2. Microbial community dynamics during the long-term operation

The dynamics of microbial community structure during the operation of the bioreactor were revealed by classifying the taxonomy of 16S rRNA gene amplicon sequencing data (Fig. 3 and Supplementary Material Table S2). During the start-up stage (days 0–87), Proteobacteria, Acidobacteriota, and Bacteroidota were the most abundant phylum-level microorganisms, accounting for an average of 48.4%, 15.73%, and 14.21%, respectively. Burkholderiales, Blastocatellales, Chitinophagales, and Rhizobiales were the dominant order-level taxa. Although microorganisms affiliated with these orders may be involved in nitrite reduction, eliminating these microorganisms (except for Burkholderiales) during long-term operations indicates that these microorganisms may not be responsible for anaerobic ethane oxidation. During the continuous stage, *Candidatus* Kerfeldbacteria, Burkholderiales, and Ignavibacteriales were the dominant order-level taxa. Interestingly, the microorganisms affiliated with *Candidatus* Kerfeldbacteria rapidly expanded the realized niche breadth with increasing influent concentration, which may have helped stabilize the microbial community, although its exact ecological significance was unclear. No known archaea capable of anaerobic ethane oxidation were detected. Thus, Burkholderiales, the dominant taxa through the whole bioreactor operation, could play a significant role in nitrite-driven anaerobic ethane oxidation.

3.3. Analysis of nitrogen and carbon metabolic pathways in microbial culture

The abundance of key genes for denitrification, assimilation nitrate reduction, anaerobic ammonium oxidation (anammox), and nitrogen fixation at metagenomic and metatranscriptomic levels have been assessed for nitrogen metabolism in the microbial culture (Fig. 4a). Nitrite reductase genes (*nirK* and *nirS*), nitric oxide

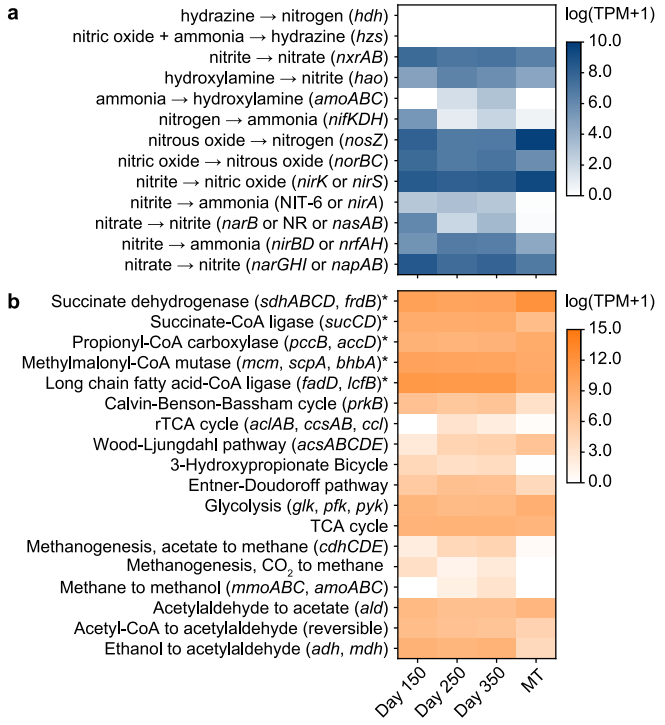

Fig. 4. Relative abundance and transcript level of genes involved in nitrogen (**a**) and carbon (**b**) metabolism pathways. Relative abundance was calculated by DiTing. The asterisks indicate that the metagenomic reads and trimmed metatranscriptomic reads were mapped onto metagenomic assembly using Bowtie2 (v2.3.2) and StringTie (v2.1.5). The relative gene abundance was determaind as GPM, and relative transcriptional abundance was determaind as TPM. MT, metatranscriptomic profiles on day 250. Nitrate reductase (NAR, *narB*); nitrate reductase (NAD(P)H) (NR); assimilatory nitrate reductase (NAS, *nasAB*); nitrite reductase (NAD(P)H) (NIT-6); ferredoxin-nitrite reductase (NiR, *nirA*); membrane-bound (NAR, *narGHI*) and periplasmic (NAP, *napAB*) dissimilatory nitrate reductases; dissimilatory nitrite reductase (ccNIR, *nrfAH*); haem-containing (cd1-NIR, *nirS*) and copper-containing (Cu-NIR, *nirK*) nitrite reductases; nitric oxide reductase (NOR, n*orBC*); nitrous oxide reductase (NOS, *nosZ*); *nif*KDH, nitrogenase; ammonia monooxygenase (AMO, *amoABC*); hydroxylamine dehydrogenase (HAO, *hao*); nitrite oxidoreductase (NXR, *nxrAB*); hydrazine synthase (HZS, *hzs*); hydrazine dehydrogenase (HDH, *hdh*); rTCA, reductive tricarboxylic acid cycle; TCA cycle, tricarboxylic acid cycle; phosphoribulokinase (PRK, *prkB*); ATP-citrate lyase (*aclAB*); citryl-CoA synthetase/ lyase (*ccsAB*/*ccl*); acetyl-CoA synthetase (ACS, acs*ABCDE*); acetyl-CoA decarbonylase/synthase (CODH/ACS, *cdhCDE*); methane/ammonia monooxygenase, (MMO/AMO, *mmoABC*/*amoABC*); alcohol/methanol dehydrogenase (ADH, *adh*; MDH, *mdh*); acetaldehyde dehydrogenase (ALDH, *ald*).

reductase genes (*norBC*), and the nitrous oxide reductase gene (*nosZ*) were detected in the three metagenomes. The high transcript levels of these genes confirmed that the microbial culture mediated the complete reduction of nitrite to N_2. The absence of genes involved in anammox indicated that the microbial culture could not undergo anammox [44], and the dynamics of the microbial community structure supported this result (Fig. 3).

Methane monooxygenases (*pmoABC*) were identified in these metagenomes (Fig. 4b). Although methane monooxygenases exhibit broad substrate specificity and can oxidize ethane under aerobic conditions [45], no transcript was detected in the metatranscriptomic profiles. Its absence indicates that methane monooxygenase did not catalyze ethane oxidation in the microbial culture. Alcohol/methanol dehydrogenase (ADH, *adh*; MDH, *mdh*) and acetyl-CoA decarbonylase/synthase (CODH/ACS, *cdhCDE*) were also expressed at low levels. Together, these results demonstrate that the oxidation of ethane to CO_2 does not likely involve methane monooxygenases.

Alkylsuccinate synthase and methyl-/ethyl-CoM reductase were implicated in the anaerobic ethane oxidation process in bacterial and archaeal-mediated systems [20,46]. No genes encoding these enzymes were identified in the metagenomic and metatranscriptomic data. However, long-chain fatty acid-CoA ligase (*fadD*, *lcfB*), methylmalonyl-CoA mutase (*mcm*), propionyl-CoA carboxylase (*pccB*, *accD*), succinate-CoA ligase (*sucCD*), and succinate dehydrogenase (*sdhABCD*, *frdB*) were identified in the metagenomic data and were expressed at high transcript levels in the metatranscriptomic data (Fig. 4b). Genes involved in beta-oxidation have also been identified in metagenomic data and expressed in metatranstriptomic data, including electron transfer flavoprotein alpha and beta subunit (*eftAB*, K03521 and K03522), acetyl-CoA acyltransferase (*fadA*, K00632; *bktB*, K00626), enoyl-CoA hydratase (*echA*, K15866), and 3-hydroxyacyl-CoA dehydrogenase (*fadN*, K07516) (Supplementary Material Data Set S1C). These results suggest an inferred pathway for the anaerobic degradation of ethane via fumarate addition and further beta-oxidation (Supplementary Material Fig. S4), consistent with that proposed for the species '*Candidatus* Alkanivorans nitratireducens' [16,47]. Meanwhile, the electrons generated by ethane oxidation could be used to reduce nitrite to N_2 through the classical denitrification pathway.

3.4. Genome recovery and metabolic function analysis of MAGs

A non-redundant set of 50 MAGs was recovered from three metagenomes. All of them had a distant genetic relationship (ANI <60%) with nitrate-driven ethane oxidizing bacteria '*Candidatus* Alkanivorans nitratireducens' [16], which may be attributed to differences in inoculums and electron receptors. Among them, nine MAGs encoded the canonical denitrification pathway (*nirK*, *nirS*, *norBC*, and *nosZ*), which can completely reduce nitrite to N_2 (Fig. 5 and Supplementary Material Data Set S2A). Based on ANI analysis and phylogenetic affiliation analysis, these nine MAGs were affiliated with three classes: Gammaproteobacteria, Xenobia, and Anaerolineae (Supplementary Material Data Sets S2B and S2C). Except for MAG_22 affiliated with an unclassified Gammaproteobacteria, the remaining MAGs all encoded genes involved in prospective anaerobic short-chain alkane (ethane/propane/n-butane) oxidation pathways (Fig. 5). These results indicated that these MAGs could have potential for nitrite-driven anaerobic ethane oxidation.

To identify the keystone taxa for nitrite-driven anaerobic ethane oxidation, the trimmed metatranscriptomic paired-end reads were mapped to MAGs with the potential for nitrite-driven anaerobic ethane oxidation. The transcripts of gene encoding nitrite reductase were detected in several MAGs (Table 1), indicating that nitrite reduction in the microbial culture was likely mediated by multiple microorganisms. Among them, MAG_36 (designated as '*Candidatus* Alkanivoras nitrosoreducens'), affiliated with the family Rhodocyclaceae and order Burkholderiales, was the most transcriptionally active, indicated by the high transcript abundance of key genes involved in nitrite reduction and prospective ethane oxidation (Table 1). Genes involved in beta-oxidation were also identified in the bacteria '*Ca.* A. nitrosoreducens' (Supplementary Material Data Set S2D). However, genes encoding alkylsuccinate synthase (*assAs*) and succinate-CoA ligase (*sucCD*) were missing in its genome. The reverse Wood–Ljungdahl pathway identified in the genome of '*Ca.* A. nitrosoreducens' was also transcriptionally active (Table 1), which suggests a potential pathway for CO_2 generation.

We successfully constructed a prospective metabolic model of nitrite-driven anaerobic ethane oxidation by the bacteria '*Ca.* A. nitrosoreducens' (Fig. 6). Ethane was determined to be oxidized to acetyl-CoA by a prospective fumarate addition pathway and beta-oxidation, consistent with the ethane oxidation pathway

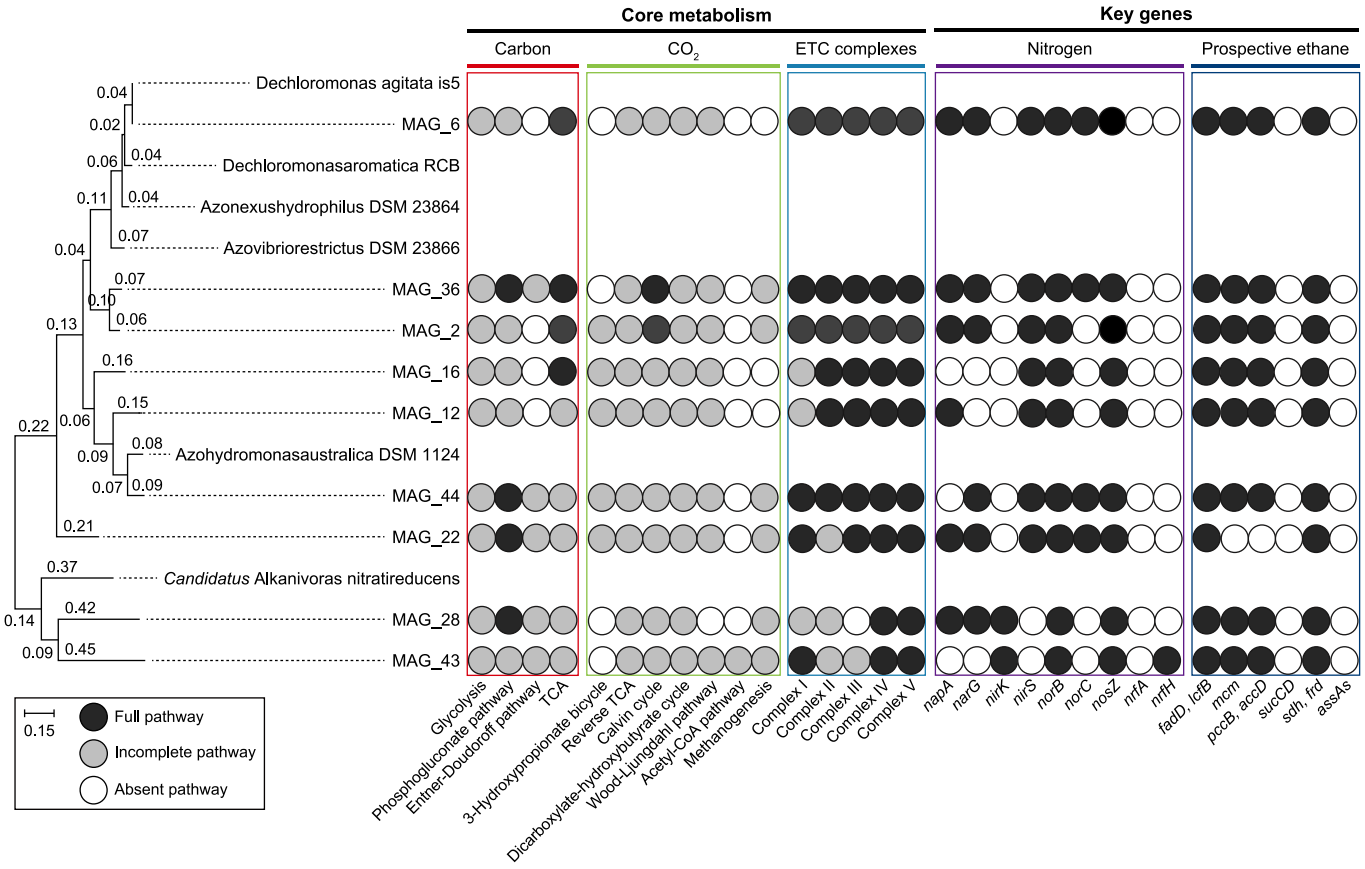

Fig. 5. Phylogenetic affiliation and metabolic potential of prospective functional MAGs. Branch lengths in the species tree were hidden if shorter than 0.01. Five neighbor public genomes and bacterial species '*Candidatus* Alkanivorans nitratireducens' were included in the species tree. ETC, electron transfer chain; TCA, tricarboxylic acid cycle; long-chain fatty acid-CoA ligase (*fadD*, *lcfB*); methylmalonyl-CoA mutase (*mcm*); propionyl-CoA carboxylase (*pccB*, *accD*); succinate-CoA ligase (*sucCD*); succinate dehydrogenase (*sdhABCD*, *frdB*); alkylsuccinate synthase (*assAs*).

Table 1
Relative abundance of genes by metatranscriptomic data mapping on MAGs.

Enzymes	MAG_12	MAG_16	MAG_22	MAG_28	MAG_36
Long-chain fatty acid-CoA ligase	66.53	764.68	5.61	3.67	3553.01
Methylmalonyl-CoA mutase	0.00	1279.96	n.a.	1.00	2296.18
Propionyl-CoA carboxylase	2.76	0.00	n.a.	0.00	5.76
Succinate-CoA ligase	n.a.	n.a.	n.a.	n.a.	n.a.
Succinate dehydrogenase	13.73	46.86	14.69	7.09	20946.94
Assimilatory nitrite reductase	3.42	12.48	807.02	0.00	1431.82
Nitrite reductase (*nirS*/*nirK*)	438.09	17.69	3.84	0.00	3.25
Nitric-oxide reductase	15.85	117.86	0.00	0.00	137.36
Nitrous-oxide reductase	4.37	0.00	0.00	39.81	93.76
5,10-methylenetetrahydrofolate reductase	0.00	97.05	0.00	0.00	0.00
Methylenetetrahydrofolate dehydrogenase	0.00	0.00	5.28	0.00	0.75
Formyltetrahydrofolate deformylase	0.00	0.00	n.a.	n.a.	1.68
Formate dehydrogenase	n.a.	268.90	0.70	0.73	180.39

n.a.: not available; the related genes were not identified in MAGs.

proposed for '*Candidatus* Alkanivorans nitratireducens' [16,47]. Then, acetyl-CoA entered the TCA cycle or reverse Wood–Ljungdahl pathway and was oxidized to CO_2. Meanwhile, nitrite was reduced to N_2 through a denitrification pathway.

4. Conclusion

This study used ethane and nitrite as substrates to enrich microbial culture capable of nitrite-driven anaerobic ethane oxidation. Based on a meta-omic analysis, '*Ca.* A. nitrosoreducens' encoded and expressed a prospective fumarate addition pathway for anaerobic ethane oxidation and a complete denitrification pathway for nitrite reduction to N_2, although the genes for ethane conversion to ethyl-succinate (*assAs*) and succinate-CoA ligase (*sucCD*) required further identification. Phylogenetic affiliation analysis showed a distant genetic relationship between '*Ca.* A. nitrosoreducens' and the previously reported '*Candidatus* Alkanivorans nitratireducens' that was capable of nitrate-driven anaerobic ethane oxidation [16], which suggests functional microbial differences in different natural environments. This study

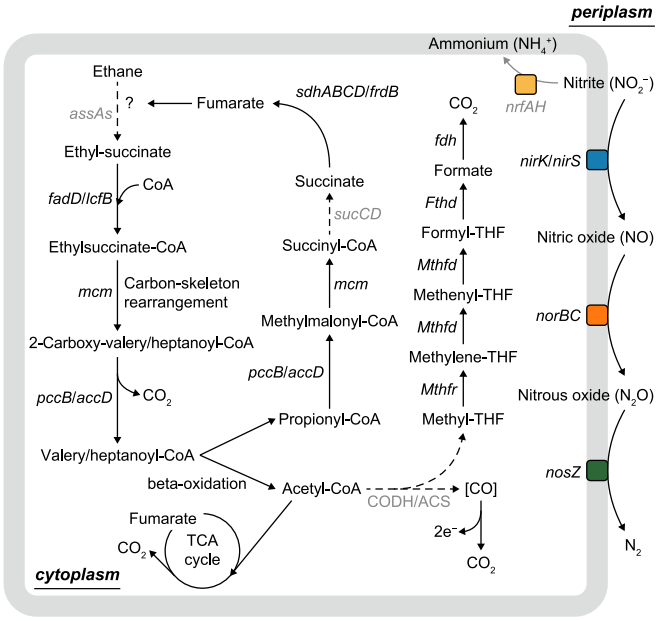

Fig. 6. Prospective metabolic model of nitrite-driven anaerobic ethane oxidation by bacteria '*Ca.* A. nitrosoreducens'. The black mark of the gene indicates that the gene has been identified in the genome, while the gray mark indicates that the gene has not been identified. TCA, tricarboxylic acid cycle; acetyl-CoA decarbonylase/synthase (CODH/ACS); alkylsuccinate synthase (*assAs*); long-chain fatty acid-CoA ligase (*fadD*, *lcfB*); methylmalonyl-CoA mutase (*mcm*); propionyl-CoA carboxylase (*pccB*, *accD*); succinate-CoA ligase (*sucCD*); succinate dehydrogenase (*sdhABCD*, *frdB*); 5,10-methylenetetrahydrofolate reductase (*Mthfr*); Methylenetetrahydrofolate dehydrogenase (*Mthfd*); Formyltetrahydrofolate deformylase (*Fthd*); Formate dehydrogenase (*fdh*); haem-containing (NirS, *nirS*) and copper-containing (NirK, *nirK*) nitrite reductases; nitric oxide reductase (NorB, n*orB*); nitrous oxide reductase (NosZ, *nosZ*); dissimilatory nitrite reductase (*nrfAH*).

offers new evidence of nitrite-driven anaerobic ethane oxidation occurring in enriched cultures from hot-spring sediment. These findings will advance the understanding of ethane and the nitrogen cycle in an environment rich in nitrite and shot-chain alkanes, highlighting the previously overlooked impact of anaerobic ethane oxidation in natural ecosystems.

Description of new species

Candidatus Alkanivoras nitrosoreducens

Etymology. Alkanivoras (al.ka.ni.vo'ras. N.L. neut. n. alkanum, alkane; L. pres. part. vorās, devouring; N.L. masc. n. ethanivoras, an alkane eater). nitrosoreducens (Ni.tro.so.re.du'cens. N.L. masc. n. nitrosum (gen. nitroso), nitrite; L. pres. part. reducens, converting to a different state; N.L. part. adj. nitrosoreducens, reducing nitrite). This name implies an organism capable of consuming alkane and reducing nitrite.

Locality. Enriched from a bioreactor inoculated with fresh hot-spring sediments collected from Tangyu, Shannxi, China.

Diagnosis. Anaerobic, alkane-oxidizing, nitrite-reducing bacteria. Mesophilic in terms of pH and thermophilic in terms of temperature (enriched at 45 ± 0.5 °C and pH 6.5–7.5).

CRediT authorship contribution statement

Cheng-Cheng Dang: Data Curation, Investigation, Methodology, Writing - Original Draft, Writing - Review & Editing. **Yin-Zhu Jin:** Data Curation, Validation. **Xin Tan:** Data Curation, Visualization, Writing - Review & Editing. **Wen-Bo Nie:** Methodology, Supervision, Writing - Review & Editing. **Yang Lu:** Methodology, Supervision, Writing - Review & Editing. **Bing-Feng Liu:** Methodology, Writing - Review & Editing. **De-Feng Xing:** Methodology, Writing - Review & Editing. **Nan-Qi Ren:** Writing - Review & Editing. **Guo-Jun Xie:** Conceptualization, Funding Acquisition, Project Administration, Resources, Supervision, Writing - Review & Editing.

Declaration of competing interest

The authors declare that they have no known competing financial interests or personal relationships that could have appeared to influence the work reported in this paper.

Acknowledgements

We acknowledge *bioinformatics* (*http://www.bioinformatics.com.cn*) and OriginLab Corporation (Northampton, Massachusetts, USA) for graphics plotting, List of Prokaryotic names with Standing in Nomenclature (LPSN, *https://lpsn.dsmz.de*) for the description and correction of new species. The authors would like to thank the Natural Science Foundation of China (Grant No. 52270032), the Fundamental Research Funds for the Central Universities (Grant No. HIT.BRET.2021014), the Fok Ying Tung Education Foundation, State Key Laboratory of Urban Water Resource and Environment, Harbin Institute of Technology (2023DX09), the Heilongjiang Nature Science Foundation (YQ2021E028) and Heilongjiang Touyan Innovation Team Program for supporting this study.

Appendix A. Supplementary data

Supplementary data to this article can be found online at https://doi.org/10.1016/j.ese.2024.100438.

References

[1] Ø. Hodnebrog, S.B. Dalsøren, G. Myhre, Lifetimes, direct and indirect radiative forcing, and global warming potentials of ethane (C_2H_6), propane (C_3H_8), and butane (C_4H_{10}), Atmos. Sci. Lett. 19 (2) (2018) e804.
[2] B. Franco, E. Mahieu, L.K. Emmons, Z.A. Tzompa-Sosa, E.V. Fischer, K. Sudo, B. Bovy, S. Conway, D. Griffin, J.W. Hannigan, K. Strong, K.A. Walker, Evaluating ethane and methane emissions associated with the development of oil and natural gas extraction in North America, Environ. Res. Lett. 11 (4) (2016) 044010.
[3] Y. Xiao, J.A. Logan, D.J. Jacob, R.C. Hudman, R. Yantosca, D.R. Blake, Global budget of ethane and regional constraints on U.S. sources, J. Geophys. Res. Atmos. 113 (D21) (2008).
[4] T. Vinciguerra, S. Yao, J. Dadzie, A. Chittams, T. Deskins, S. Ehrman, R.R. Dickerson, Regional air quality impacts of hydraulic fracturing and shale natural gas activity: evidence from ambient VOC observations, Atmos. Environ. 110 (2015) 144–150.
[5] S. Schwietzke, W.M. Griffin, H.S. Matthews, L.M.P. Bruhwiler, Natural gas fugitive emissions rates constrained by global atmospheric methane and ethane, Environ. Sci. Technol. 48 (14) (2014) 7714–7722.
[6] Z.A. Tzompa-Sosa, E. Mahieu, B. Franco, C.A. Keller, A.J. Turner, D. Helmig, A. Fried, D. Richter, P. Weibring, J. Walega, T.I. Yacovitch, S.C. Herndon, D.R. Blake, F. Hase, J.W. Hannigan, S. Conway, K. Strong, M. Schneider, E.V. Fischer, Revisiting global fossil fuel and biofuel emissions of ethane, J. Geophys. Res. Atmos. 122 (4) (2017) 2493–2512.
[7] D.I. Foustoukos, W.E. Seyfried, Hydrocarbons in hydrothermal vent fluids: the role of chromium-bearing catalysts, Science 304 (5673) (2004) 1002–1005.
[8] M. Song, F. Schubotz, M.Y. Kellermann, C.T. Hansen, W. Bach, A.P. Teske, K.U. Hinrichs, Formation of ethane and propane via abiotic reductive conversion of acetic acid in hydrothermal sediments, Proc. Natl. Acad. Sci. U. S. A. 118 (47) (2021).
[9] K.-U. Hinrichs, J.M. Hayes, W. Bach, A.J. Spivack, L.R. Hmelo, N.G. Holm, C.G. Johnson, S.P. Sylva, Biological formation of ethane and propane in the deep marine subsurface, Proc. Natl. Acad. Sci. USA 103 (40) (2006) 14684–14689.
[10] M.R. Gomez-Garcia, M. Davison, M. Blain-Hartnung, A.R. Grossman, D. Bhaya, Alternative pathways for phosphonate metabolism in thermophilic cyanobacteria from microbial mats, ISME J. 5 (1) (2011) 141–149.
[11] T. Saito, Y. Yokouchi, K. Kawamura, Distributions of C2-C6 hydrocarbons over the western north pacific and eastern Indian ocean, Atmos. Environ. 34 (25)

(2000) 4373–4381.
[12] V. Mastalerz, G.J. de Lange, A. Dählmann, Differential aerobic and anaerobic oxidation of hydrocarbon gases discharged at mud volcanoes in the Nile deep-sea fan, Geochem. Cosmochim. Acta 73 (13) (2009) 3849–3863.
[13] A. Stadnitskaia, M.K. Ivanov, V. Blinova, R. Kreulen, T.C.E. van Weering, Molecular and carbon isotopic variability of hydrocarbon gases from mud volcanoes in the Gulf of Cadiz, NE Atlantic, Mar. Petrol. Geol. 23 (3) (2006) 281–296.
[14] M.M. Adams, A.L. Hoarfrost, A. Bose, S.B. Joye, P.R. Girguis, Anaerobic oxidation of short-chain alkanes in hydrothermal sediments: potential influences on sulfur cycling and microbial diversity, Front. Microbiol. 4 (2013) 110.
[15] A. Bose, D.R. Rogers, M.M. Adams, S.B. Joye, P.R. Girguis, Geomicrobiological linkages between short-chain alkane consumption and sulfate reduction rates in seep sediments, Front. Microbiol. 4 (2013) 386.
[16] M. Wu, J. Li, C.Y. Lai, A.O. Leu, S. Sun, R. Gu, D.V. Erler, L. Liu, L. Li, G.W. Tyson, Z. Yuan, S.J. McIlroy, J. Guo, Nitrate-driven anaerobic oxidation of ethane and butane by bacteria, ISME J. 18 (1) (2024).
[17] C.J. Hahn, R. Laso-Perez, F. Vulcano, K.M. Vaziourakis, R. Stokke, I.H. Steen, A. Teske, A. Boetius, M. Liebeke, R. Amann, K. Knittel, G. Wegener, "Candidatus Ethanoperedens," a thermophilic genus of archaea mediating the anaerobic oxidation of ethane, mBio 11 (2) (2020) e00600–e00620.
[18] R. Laso-Perez, C. Hahn, D.M. van Vliet, H.E. Tegetmeyer, F. Schubotz, N.T. Smit, T. Pape, H. Sahling, G. Bohrmann, A. Boetius, K. Knittel, G. Wegener, Anaerobic degradation of non-methane alkanes by "Candidatus methanoliparia" in hydrocarbon seeps of the gulf of Mexico, mBio 10 (4) (2019).
[19] S.C. Chen, N. Musat, O.J. Lechtenfeld, H. Paschke, M. Schmidt, N. Said, D. Popp, F. Calabrese, H. Stryhanyuk, U. Jaekel, Y.G. Zhu, S.B. Joye, H.H. Richnow, F. Widdel, F. Musat, Anaerobic oxidation of ethane by archaea from a marine hydrocarbon seep, Nature 568 (7750) (2019) 108–111.
[20] R. Singh, M.S. Guzman, A. Bose, Anaerobic oxidation of ethane, propane, and butane by marine microbes: a mini review, Front. Microbiol. 8 (2056) (2017).
[21] J.N. Galloway, A.R. Townsend, J.W. Erisman, M. Bekunda, Z. Cai, J.R. Freney, L.A. Martinelli, S.P. Seitzinger, M.A. Sutton, Transformation of the nitrogen cycle: recent trends, questions, and potential solutions, Science 320 (5878) (2008) 889–892.
[22] K.C. Costa, J.B. Navarro, E.L. Shock, C.L. Zhang, D. Soukup, B.P. Hedlund, Microbiology and geochemistry of great boiling and mud hot springs in the United States Great Basin, Extremophiles 13 (3) (2009) 447–459.
[23] T.J. Vick, J.A. Dodsworth, K.C. Costa, E.L. Shock, B.P. Hedlund, Microbiology and geochemistry of little hot creek, a hot spring environment in the long valley caldera, Geobiology 8 (2) (2010) 140–154.
[24] B.J. Callahan, P.J. McMurdie, M.J. Rosen, A.W. Han, A.J. Johnson, S.P. Holmes, DADA2: high-resolution sample inference from Illumina amplicon data, Nat. Methods 13 (7) (2016) 581–583.
[25] C. Quast, E. Pruesse, P. Yilmaz, J. Gerken, T. Schweer, P. Yarza, J. Peplies, F.O. Glöckner, The SILVA ribosomal RNA gene database project: improved data processing and web-based tools, Nucleic Acids Res. 41 (Database issue) (2013) D590–D596.
[26] T. Chen, X. Chen, S. Zhang, J. Zhu, B. Tang, A. Wang, L. Dong, Z. Zhang, C. Yu, Y. Sun, L. Chi, H. Chen, S. Zhai, Y. Sun, L. Lan, X. Zhang, J. Xiao, Y. Bao, Y. Wang, Z. Zhang, W. Zhao, The genome sequence archive family: toward explosive data growth and diverse data types, Dev. Reprod. Biol. 19 (4) (2021) 578–583.
[27] C.-N.M.a. Partners, Database Resources of the national genomics data center, China national center for bioinformation in 2023, Nucleic Acids Res. 51 (D1) (2023) D18–D28.
[28] A.P. Arkin, R.W. Cottingham, C.S. Henry, N.L. Harris, R.L. Stevens, S. Maslov, P. Dehal, D. Ware, F. Perez, S. Canon, M.W. Sneddon, M.L. Henderson, W.J. Riehl, D. Murphy-Olson, S.Y. Chan, R.T. Kamimura, S. Kumari, M.M. Drake, T.S. Brettin, E.M. Glass, D. Chivian, D. Gunter, D.J. Weston, B.H. Allen, J. Baumohl, A.A. Best, B. Bowen, S.E. Brenner, C.C. Bun, J.M. Chandonia, J.M. Chia, R. Colasanti, N. Conrad, J.J. Davis, B.H. Davison, M. DeJongh, S. Devoid, E. Dietrich, I. Dubchak, J.N. Edirisinghe, G. Fang, J.P. Faria, P.M. Frybarger, W. Gerlach, M. Gerstein, A. Greiner, J. Gurtowski, H.L. Haun, F. He, R. Jain, M.P. Joachimiak, K.P. Keegan, S. Kondo, V. Kumar, M.L. Land, F. Meyer, M. Mills, P.S. Novichkov, T. Oh, G.J. Olsen, R. Olson, B. Parrello, S. Pasternak, E. Pearson, S.S. Poon, G.A. Price, S. Ramakrishnan, P. Ranjan, P.C. Ronald, M.C. Schatz, S.M.D. Seaver, M. Shukla, R.A. Sutormin, M.H. Syed, J. Thomason, N.L. Tintle, D. Wang, F. Xia, H. Yoo, S. Yoo, D. Yu, KBase: the United States department of energy systems biology knowledgebase, Nat. Biotechnol. 36 (7) (2018) 566–569.
[29] C.X. Xue, H. Lin, X.Y. Zhu, J. Liu, Y. Zhang, G. Rowley, J.D. Todd, M. Li, X.H. Zhang, DiTing: a pipeline to infer and compare biogeochemical pathways from metagenomic and metatranscriptomic data, Front. Microbiol. 12 (2021) 698286.
[30] W.B. Langdon, Performance of genetic programming optimised Bowtie2 on genome comparison and analytic testing (GCAT) benchmarks, BioData Min. 8 (1) (2015) 1.
[31] M. Pertea, D. Kim, G.M. Pertea, J.T. Leek, S.L. Salzberg, Transcript-level expression analysis of RNA-seq experiments with HISAT, StringTie and Ballgown, Nat. Protoc. 11 (9) (2016) 1650–1667.
[32] M.R. Olm, C.T. Brown, B. Brooks, J.F. Banfield, dRep: a tool for fast and accurate genomic comparisons that enables improved genome recovery from metagenomes through de-replication, ISME J. 11 (12) (2017) 2864–2868.
[33] T. Seemann, Prokka: rapid prokaryotic genome annotation, Bioinformatics 30 (14) (2014) 2068–2069.
[34] T. Brettin, J.J. Davis, T. Disz, R.A. Edwards, S. Gerdes, G.J. Olsen, R. Olson, R. Overbeek, B. Parrello, G.D. Pusch, M. Shukla, J.A. Thomason 3rd, R. Stevens, V. Vonstein, A.R. Wattam, F. Xia, RASTtk: a modular and extensible implementation of the RAST algorithm for building custom annotation pipelines and annotating batches of genomes, Sci. Rep. 5 (2015) 8365.
[35] P.A. Chaumeil, A.J. Mussig, P. Hugenholtz, D.H. Parks, GTDB-Tk: a toolkit to classify genomes with the Genome Taxonomy Database, Bioinformatics 36 (6) (2019) 1925–1927.
[36] C. Jain, L.M. Rodriguez-R, A.M. Phillippy, K.T. Konstantinidis, S. Aluru, High throughput ANI analysis of 90K prokaryotic genomes reveals clear species boundaries, Nat. Commun. 9 (1) (2018) 5114.
[37] R.C. Edgar, Search and clustering orders of magnitude faster than BLAST, Bioinformatics 26 (19) (2010) 2460–2461.
[38] M. Shaffer, M.A. Borton, B.B. McGivern, A.A. Zayed, Sabina L. La Rosa, L.M. Solden, P. Liu, A.B. Narrowe, J. Rodríguez-Ramos, B. Bolduc, M.C. Gazitúa, R.A. Daly, G.J. Smith, D.R. Vik, P.B. Pope, M.B. Sullivan, S. Roux, Kelly C. Wrighton, DRAM for distilling microbial metabolism to automate the curation of microbiome function, Nucleic Acids Res. 48 (16) (2020) 8883–8900.
[39] K. Tamura, G. Stecher, S. Kumar, MEGA11: molecular evolutionary genetics analysis version 11, Mol. Biol. Evol. 38 (7) (2021) 3022–3027.
[40] A.M. Bolger, M. Lohse, B. Usadel, Trimmomatic: a flexible trimmer for Illumina sequence data, Bioinformatics 30 (15) (2014) 2114–2120.
[41] S. Andrews, FASTQC. A quality control tool for high throughput sequence data. http://www.bioinformatics.babraham.ac.uk/projects/fastqc/, 2014.
[42] APHA, Standard Methods for the Examination of Water and Wastewater, 23rd ed., American Pubic Health Association, Washington, 2017.
[43] L. Zhou, C.E. Boyd, Comparison of Nessler, phenate, salicylate and ion selective electrode procedures for determination of total ammonia nitrogen in aquaculture, Aquaculture 450 (2016) 187–193.
[44] B. Kartal, W.J. Maalcke, N.M. de Almeida, I. Cirpus, J. Gloerich, W. Geerts, H. den Camp, H.R. Harhangi, E.M. Janssen-Megens, K.J. Francoijs, H.G. Stunnenberg, J.T. Keltjens, M.S.M. Jetten, M. Strous, Molecular mechanism of anaerobic ammonium oxidation, Nature 479 (7371) (2011) 127–U159.
[45] S.H. Oh, I.Y. Hwang, O.K. Lee, W. Won, E.Y. Lee, Development and optimization of the biological conversion of ethane to ethanol using whole-cell methanotrophs possessing methane monooxygenase, Molecules 24 (2019), https://doi.org/10.3390/molecules24030591.
[46] C.J. Hahn, O.N. Lemaire, J. Kahnt, S. Engilberge, G. Wegener, T. Wagner, Crystal structure of a key enzyme for anaerobic ethane activation, Science 373 (6550) (2021) 118. +.
[47] M. Wu, J. Li, A.O. Leu, D.V. Erler, T. Stark, G.W. Tyson, Z. Yuan, S.J. McIlroy, J. Guo, Anaerobic oxidation of propane coupled to nitrate reduction by a lineage within the class Symbiobacteriia, Nat. Commun. 13 (1) (2022) 6115.